Breakdown Walkout in Polarization-Doped Vertical GaN Diodes

Elena Fabris, Carlo De Santi, Alessandro Caria, Kazuki Nomoto, Zongyang Hu, Wenshen Li, Xiang Gao, Debdeep Jena, Huili Grace Xing, Gaudenzio Meneghesso, *Fellow, IEEE*, Enrico Zanoni, *Fellow IEEE*, and Matteo Meneghini, *Senior Member, IEEE*

***Abstract*—We demonstrate the avalanche capability and the existence of breakdown walkout in GaN-on-GaN vertical devices with polarization doping. By means of combined electrical and optical characterization, we demonstrate the following original results: 1) vertical p-n junctions with polarization doping have avalanche capability; 2) stress in avalanche regime induces an increase in breakdown voltage, referred to as breakdown walkout; 3) this process is fully-recoverable, thus being related to a trapping mechanism; 4) temperature-dependent measurements of the breakdown walkout identify C_N defects responsible for this process; and 5) capacitance deep level transient spectroscopy (C-DLTS) and deep level optical spectroscopy (DLOS) confirm the presence of residual carbon in the devices under test. A possible model to explain the avalanche walkout is then proposed.**

***Index Terms*—Avalanche breakdown, breakdown walkout, carbon, gallium nitride, p-n junction, vertical diodes, widebandgap semiconductors.**

I. Introduction

GaN p-n junctions are the basic units of vertical power devices; the study of p-n diodes permits to extract the fundamental information on material/device physics, especially related to avalanche and impact ionization [1]–[5].

The breakdown ruggedness is of fundamental importance for power applications, and, therefore, the avalanche capability of the GaN-on-GaN vertical diodes has to be investigated [6]. In addition, polarization doping has been recently proposed as an effective alternative to impurity doping for the fabrication of high-performance GaN-based vertical devices, and initial experiments have been carried out [7]–[11]. The electrical performance and the stability of these devices still have to be analyzed in detail.

To significantly advance the understanding in this field, this article presents an extensive analysis of the stability of polarization-doped graded AlGaN vertical p-n diodes in avalanche regime. We build on a previous conference presentation on the topic [12], and we add a substantial contribution to the analysis of the defects related to the breakdown walkout.

This article demonstrates that: in this early generation of GaN-based p-n diodes with polarization doping, 1) they are avalanche capable; 2) the breakdown voltage (BDV) moves to more negative values when the devices are submitted to a reverse current stress for a long time, i.e. the devices show a breakdown walkout process; 3) the breakdown walkout is recoverable and related to trapping processes. Temperature-dependent measurements indicate that this process could be due to carbon acceptor, which is attributed to carbon on nitrogen sites (C_N) [13]; and 4) capacitance deep level transient spectroscopy (C-DLTS) and deep level optical spectroscopy (DLOS) confirm a high level of residual carbon in the devices, suggesting that the observed breakdown walkout is most likely dominated by the un-intended carbon present in the device epitaxy, and not by the polarization doping. Finally, a model that can explain the experimental data and the role of residual carbon causing the breakdown walkout in the analyzed diodes is proposed.

II. Device Structure

Fig. 1 shows the structure of the diodes under test. The devices are based on a polarization-doped AlGaN vertical p-n junction grown by metal-organic chemical vapor deposition (MOCVD). By grading the Al composition, it is possible to enhance both n-type and p-type conductivity compared to the impurity-doped case, and to achieve no-carrier freeze-out, thanks to the electric field activated doping. In fact, it is worth noting that moderately doped GaN:Mg suffers from partial freeze-out even at room temperature due to its large activation energy ~160–200 meV [14], [15] (e.g. ~1% Mg acceptors are ionized at room temperature to provide mobile holes). Considering high-frequency power electronics (> 10 kHz) for which the wide bandgap semiconductors are suitable, the time constant necessary to ionize

Manuscript received May 13, 2019; revised August 30, 2019; accepted September 18, 2019. Date of publication October 14, 2019; date of current version October 29, 2019. The review of this article was arranged by Editor K. J. Chen. *(Corresponding author: Elena Fabris.)*

E. Fabris, C. De Santi, A. Caria, G. Meneghesso, E. Zanoni, and M. Meneghini are with the Department of Information Engineering, University of Padova, 35122 Padua, Italy (e-mail: elena.fabris@dei.unipd.it; matteo.meneghini@dei.unipd.it).

K. Nomoto, Z. Hu, and W. Li are with the School of Electrical and Computer Engineering, Cornell University, Ithaca, NY 14853 USA.

X. Gao is with IQE RF LLC, Somerset, NJ 08873 USA.

D. Jena and H. G. Xing are with the School of Electrical and Computer Engineering, Department of Materials Science and Engineering, Kavli Institute at Cornell for Nanoscience, Cornell University, Ithaca, NY 14853 USA.

Color versions of one or more of the figures in this article are available online at http://ieeexplore.ieee.org.

Digital Object Identifier 10.1109/TED.2019.2943014

0018-9383 © 2019 IEEE. Personal use is permitted, but republication/redistribution requires IEEE permission.
See http://www.ieee.org/publications_standards/publications/rights/index.html for more information.

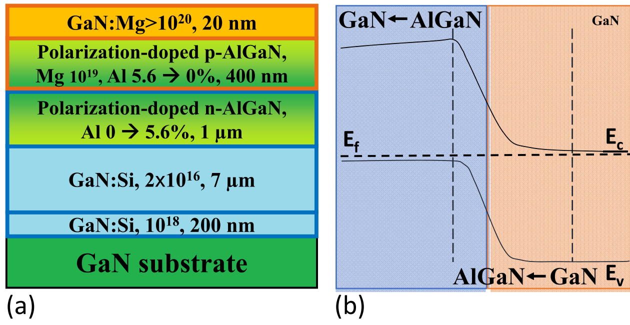

Fig. 1. (a) Structure of the device under test. (b) Energy band diagram of the polarization-induced AlGaN vertical p-n diode.

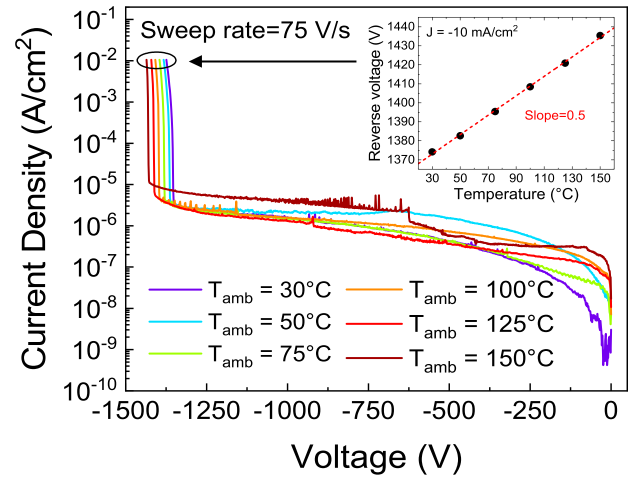

Fig. 2. I–V characteristics at different temperatures. Inset: dependence of BDV at 10^{-2} A/cm^2 on temperature; the temperature coefficient is positive with a slope of 0.5 V/°C.

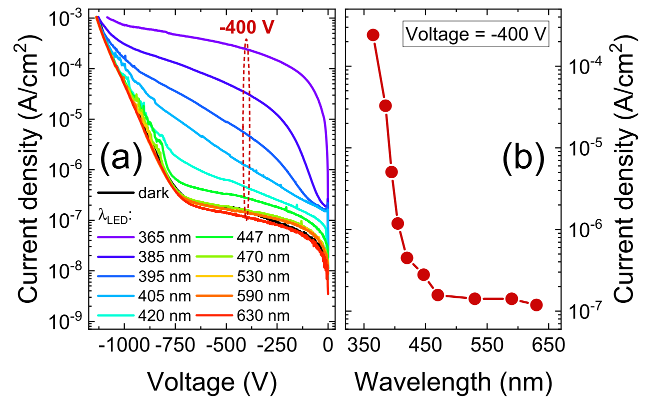

Fig. 3. (a) I–V characteristics under external illumination. (b) Dependence of the current density at −400 V on the wavelength of the external illumination.

Mg leads to the frequency dispersion [16], i.e. dynamic degradation of breakdown and/or dynamic R_{on}. These are the advantages of polarization doping for power semiconductor devices under application conditions. Moreover, the larger bandgap of AlGaN allows to reach a higher breakdown field, resulting in an improvement of the breakdown properties [9].

The structure, grown on a GaN substrate, consists of an Si-doped n$^-$ GaN layer (200 nm) with doping N_D $\sim 10^{18}$ cm^{-3}, a Si-doped n GaN layer (7 μm) with doping N_D $\sim 2 \times 10^{16}$ cm^{-3}, an n-type linearly graded AlGaN layer with the Al composition graded up from 0% to 5.6% (1 μm), a p-type linearly graded AlGaN layer with the opposite Al composition gradient (from 5.6% to 0%) (0.4 μm), and an Mg-doped p GaN layer (20 nm) with doping higher than 10^{20} cm^{-3}. The polarization charge in the p-layer is $\sim 6.5 \times 10^{16}$ cm^{-3}, and in the n-layer is $\sim 2.6 \times 10^{16}$ cm^{-3}. The devices presented in this article are the very first generation of polarization-doped devices of Cornell University; neither the design nor the growth conditions were optimized. Nonetheless, the presence of Al in the polarization-doped layers and the presence of carbon in the drift layer make these devices very interesting to study breakdown behavior under these influences. The analyzed diodes were optimized for high BDV through the use of a field plate [1], [6].

III. Measurement Results and Discussion

A. Avalanche Breakdown

The reverse characteristics of the p-n diode at different temperatures are shown in Fig. 2 (all measurements are carried out on the very same sample). The results indicate a sudden increase in the leakage current for reverse voltages higher than 1370 V. Assuming a first-order 1-D model and a complete depletion of the drift layer, this value corresponds to a critical field around 1.9 MV/cm. The BDVs at different temperatures show a positive temperature coefficient, with a slope (0.5 V/°C) consistent with a previous report [3]–[5], [17] (see inset in Fig. 2). A positive temperature coefficient of the BDV proves that the breakdown mechanism in reverse biased diodes could be related to impact-ionization initiated avalanche [3]–[5], [17]–[19].

To investigate the reverse leakage below the onset of avalanche and to understand if the increase in the current was related to an avalanche process or to Poole–Frenkel emission, reverse current measurements were carried out under external illumination (Fig. 3). The light enters the sample, thanks to the waveguiding and scattering. The measurements are calibrated, i.e. we calculated the current of each LED in order to have the same photon flux to the device active area. Fig. 3(a) shows an increase in the leakage current in the preavalanche region when the devices are illuminated with monochromatic light. This effect is observed 1) when the devices are illuminated with a wavelength of 365 nm (that corresponds to a photon energy equivalent to the energy gap of the GaN), indicating that the light is able to reach the active region and limited band-to-band absorption occurs and 2) also for subbandgap excitation (wavelength longer than 365 nm).

Two different processes may lead to the observed increase in the leakage with subbandgap excitation. One is the light-induced detrapping from deep defects. However, the BDV and the resistance in the high current region are not influenced by the external illumination, and, thus, this hypothesis is excluded. A second likely explanation is that the increase

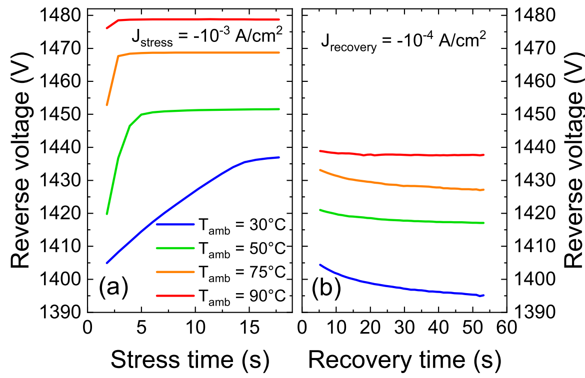

Fig. 4. Time-dependence of breakdown walkout at different temperatures. The BDV (a) increases during the stress time ($J_{stress} = -10^{-3}$ A/cm^2) and (b) recovers during the recovery time ($J_{recovery} = -10^{-4}$ A/cm^2).

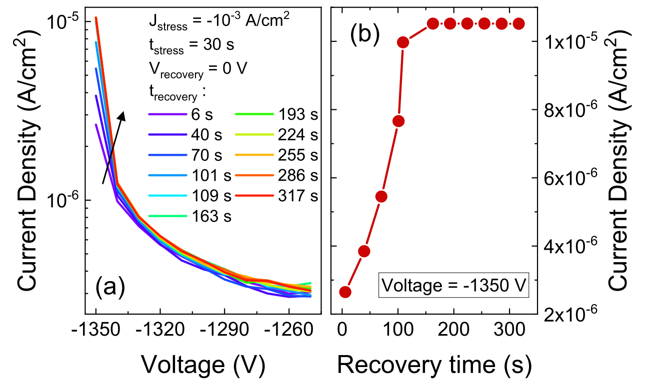

Fig. 5. (a) *I–V* characteristics carried out at different recovery times after 30 s of reverse-bias stress. (b) Full recovery of the current density during the recovery phase.

in the leakage current in the preavalanche region is due to the Franz–Keldysh effect, i.e. due to the presence of exponential band tails extending into the bandgap caused by local potential variations [20]. The Franz–Keldysh effect reduces the energy for photon absorption, thus resulting in an increased leakage current, also with subbandgap excitation, for the high electric field. This hypothesis is consistent with very recent articles on the topic [21], [12].

B. Breakdown Walkout

In this section, we investigated the stability of the avalanche voltage and demonstrated the existence of breakdown walkout in vertical GaN devices.

The breakdown walkout consists in the shift of the BDV to higher negative values. Recently, this process was demonstrated for vertical GaN devices for the first time by our group [12], however, more detailed analysis are needed. It was observed in silicon (Si) p-n junctions [22] and in AlGaAs/GaAs high electron mobility transistors (HEMTs) [23], however, both in Si p-n junctions and AlGaAs/GaAs HEMTs, the drift of the voltage was irreversible. The breakdown walkout was demonstrated to be reversible by Bin Tang and Hsin [24] in AlGaAs/InGaAs pseudomorphic HEMTs. Tang concluded that the breakdown walkout was due to the detrapping process at the interface between the gate metal and semiconductor, and in AlGaAs surface [24].

Fig. 4(a) shows the presence of breakdown walkout in GaN-on-GaN p-n junctions; the BDV moves to higher negative values when the device is submitted to a reverse current stress at 1 mA/cm^2 at different temperatures (30 °C, 50 °C, 70 °C, and 90 °C). This time-dependent process becomes faster at higher temperatures and results in a maximum voltage variation of 32 V at 30 °C. As shown in Figs. 4(b) and 5, this mechanism is not permanent and the avalanche voltage recovers in a few hundreds of seconds. The recovery of the BDV was analyzed by means of two different measurements: the first one [Fig. 4(b)] consists in monitoring the variation in the reverse voltage when a constant current density ($J_{recovery} = -10^{-4}$ A/cm^2) is applied; the second one (Fig. 5) consists in maintaining the device in a rest condition with a recovery voltage of 0 V, and in monitoring the variation in the reverse voltage/current density in avalanche regime by means of fast *I–V* characterization.

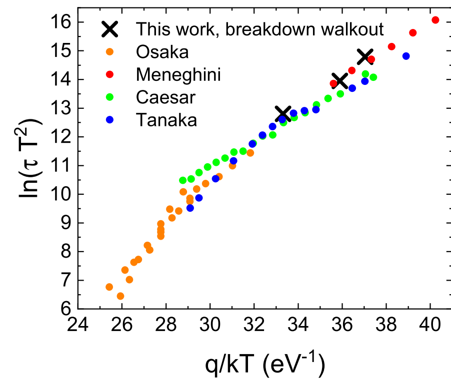

Fig. 6. Comparison between literature and the Arrhenius plot of the breakdown walkout process. The activation energy of the identified trap is $E_a = 0.52$ eV. The time constant τ is measured in second and the temperature *T* in kelvin.

By using stretched-exponential fits of the recovery transients of the BDV at different temperatures shown in Fig. 4(b), an activation energy $E_a = 0.52$ eV was found. In Fig. 6, we reported the Arrhenius plot of the extracted deep level (black symbols); we can see that the signature of the extracted deep level is compatible with other signatures reported in the literature [25]–[28]. Based on this comparison with the literature, the walkout breakdown may be related to the charge trapping process due to the presence of carbon impurities on nitrogen sites (C_N). Typically, C_N has an activation energy E_a ~0.8–0.9 eV [13]; the lower E_a found here may be due to the Poole-Frenkel effect, that lowers the potential barrier when a high electric field is present [29].

In the analyzed devices, no intentional carbon doping is present but secondary ion mass spectroscopy (SIMS) reveals a residual concentration of $\sim 2 \times 10^{16}$ cm^{-3} in the GaN:Si drift layer and $\sim 6 \times 10^{16}$ cm^{-3} in the AlGaN polarization-doped drift layer for the analyzed devices (see Fig. 7) due to un-optimized growth of both the impurity-doped and graded AlGaN layers in this generation of device wafers, and this high level of carbon incorporation makes these devices particularly interesting for this article.

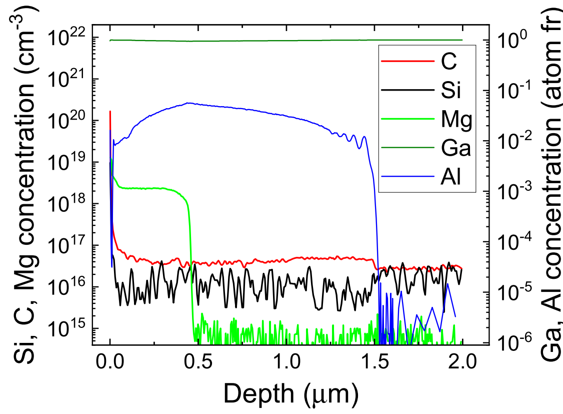

Fig. 7. SIMS data of the devices under test. The carbon level in this generation of un-optimized wafer growth is about 2–4 × 10^{16} cm^{-3}, higher than our later generations where the carbon level is about 10^{16} cm^{-3} or lower (for example, see devices in [3]).

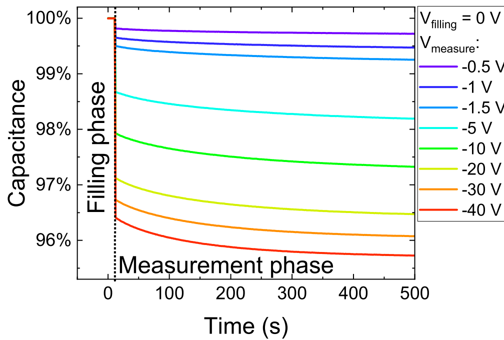

Fig. 8. C-DLTS tests at different measured voltage. All data were normalized with respect to the capacitance value in the filling phase.

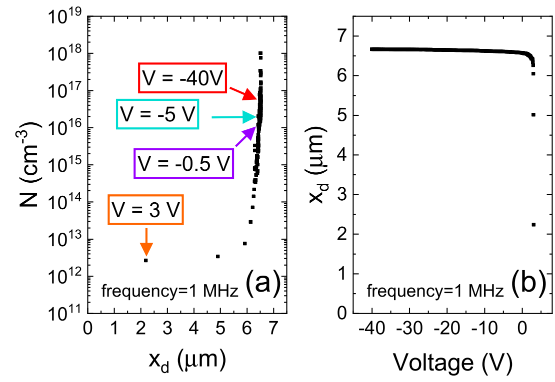

Fig. 9. Apparent free charge density N versus depletion region x_d (a) and depletion region x_d versus voltage (b) carried out during a capacitance measurement at 1 MHz.

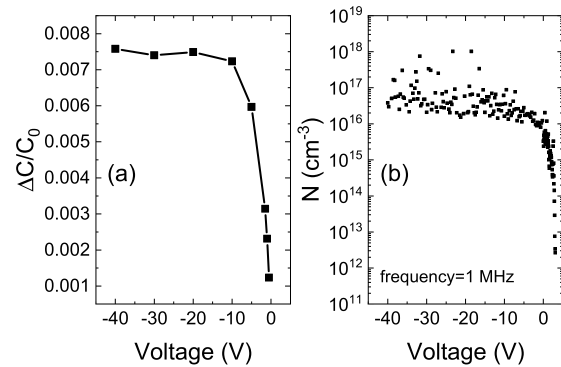

Fig. 10. Comparison between the amplitude of the transient (a) and apparent free charge density (carried out at 1 MHz) (b). $\Delta C/C$ values are calculated with respect to the first point of the measurement phase (that is highlighted in Fig. 8 by using the dashed line).

C. C-DLTS and DLOS

In order to confirm that the deep level identified with the breakdown walkout measurements is related to C_N, C-DLTS and DLOS measurements were carried out.

C-DLTS is based on filling the defects in the depletion region by applying a filling voltage (V_{filling}) and then observing the corresponding detrapping kinetics by analyzing the capacitance transient at a measured voltage (V_{measure}) [30]. The measurements are repeated at different temperatures to extract the Arrhenius plot. We developed a new setup that can reach measured voltages up to ±40 V. Fig. 8 shows the results of the measurements carried out at different voltages; the aims of these measurements were to choose the optimal voltage to observe the thermal release of the carriers from the defects, i.e. a voltage that induces a change in the capacitance that has an exponential behavior, a detectable amplitude, and a time constant concluded in the temporal range under investigation, and to make sure that the detected transient is not related to the surface states or parasitic effects. In fact, by using different voltages, it is possible to analyze different active volumes. By analyzing Fig. 8, it is possible to notice that when a more negative voltage is applied, the amplitude of the capacitance transient (which is proportional to the total number of deep levels) increases, confirming that the transient is due to a minority carrier trap distributed in the whole region near the junction.

To better understand which part of the device is probed by the edge of the space charge region at every measured voltage, capacitance-voltage measurements were carried out at 1 MHz, and the related apparent charge profiles were extracted (Fig. 9). The results indicate that the region under analysis is the interface between the unintentionally compensated GaN:Si drift layer and a highly Si-doped buffer layer. As shown in Fig. 10(a), the deep level concentration is the highest closer to this interface and becomes negligible deeper into the highly-doped region. By comparing this trend with one of the apparent free charge density extracted from the C–V measurements [Fig. 10(b)], it is possible to notice that the two follow the same trend. This indicates that the detected deep levels are compensating the Si doping and are present almost in the same concentration as the silicon in the lightly-doped region (see Fig. 7), suggesting that the carbon is the impurity generating in the deep level signal. It is worth noting that the C and Si levels reported in the SIMS data (Fig. 7) are comparable in the devices, suggesting that the drift region is well compensated. This is confirmed by the C–V measurements. We can observe that the estimated N_d–N_a based on the C–V measurements is 3 × 10^{12} cm^{-3} and the depletion depth is close to the interface between the 7-μm compensated GaN:Si

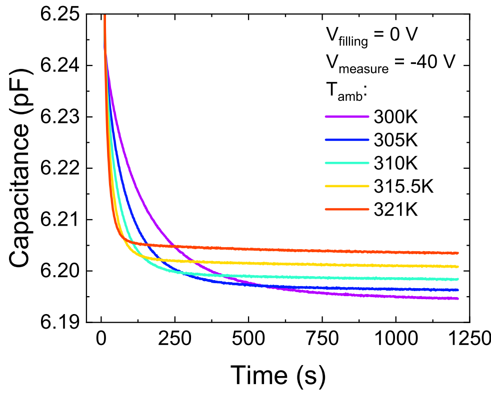

Fig. 11. C-DLTS tests at different temperatures.

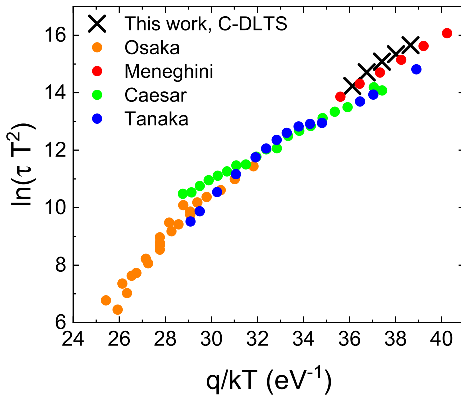

Fig. 12. Comparison between literature and the Arrhenius plot of the C-DLTS measurements. The activation energy of the identified trap is $E_a = 0.79$ eV.

drift layer and a highly doped GaN buffer layer at low reverse bias [Fig. 9(a)].

In order to confirm the assumption that the detected deep levels could be ascribed to C_N, Fig. 11 shows the capacitance transients at different temperatures; by analyzing these transients, the Arrhenius plot reported in Fig. 12 was obtained. The comparison of the signature of the trap detected by the C-DLTS measurements with the previous article in the literature confirms the possible presence of C_N, as previously assumed with the breakdown walkout measurements.

Moreover, DLOS was used to roughly estimate the concentration of residual carbon in the device, which was found to be around 1.7×10^{16} cm^{-3}. During the DLOS measurement, the capacitance transient is monitored; at a given moment, the device is illuminated with a monochromatic light, resulting in the emission of trapped electrons through the absorption of photons, causing a variation in the junction capacitance. When the capacitance reaches the steady-state value, the light is turned off and the capacitance gradually returns to the initial value (Fig. 13) [31]. This technique allows to investigate the presence and density of traps across the whole bandgap by using photon energies ranging from 1.5 to 3.65 eV. Results of DLOS measurements are shown in Figs. 14 and 15. As can be noticed in Fig. 15(b), a change in the slope of the steady-state photocapacitance spectrum is visible at 2.46 eV, indicating an

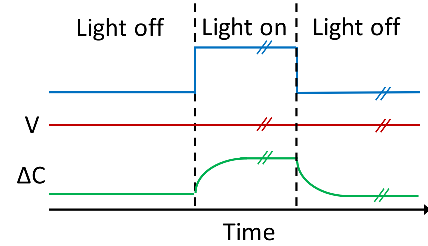

Fig. 13. Schematic of a DLOS measurement.

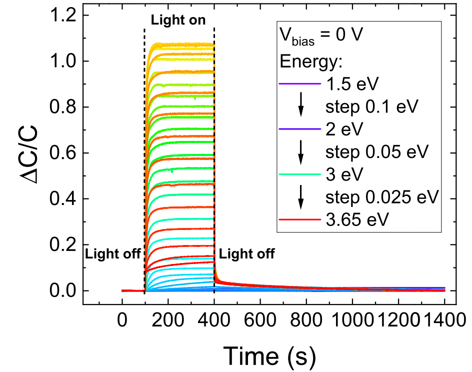

Fig. 14. Capacitance transients obtained using different wavelengths of monochromatic incident light during a DLOS measurement.

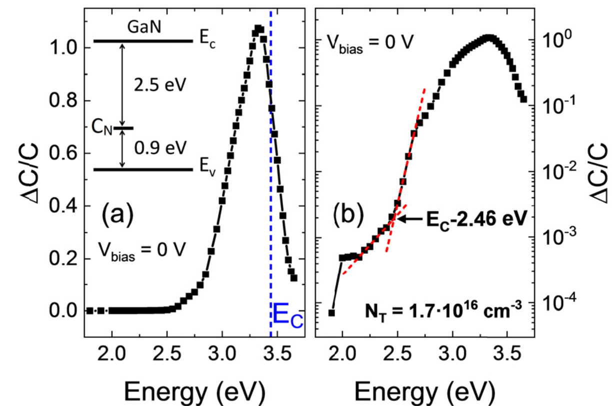

Fig. 15. Steady-state photocapacitance spectrum in (a) linear scale and (b) semi-log scale.

emission process of carriers from a deep level located 2.46 eV below the conduction band [32]. The energy of the deep level corresponds to that of C_N [13], confirming the hypothesis of the presence of residual carbon in the p-n junctions under test.

D. Avalanche Walkout Model

In the previous sections, we have demonstrated that the avalanche walkout is related to the presence of residual carbon within the devices. Now, we discuss the physical origin of this process, by interpreting the data discussed above. The free carriers travel in the space-charge region of a reverse-biased p-n junction, on the average, a distance λ (mean-free path) before exchanging energy by means of vibrations (i.e. phonons) with the lattice, dopant atoms, crystal defects, or unintentional impurities.

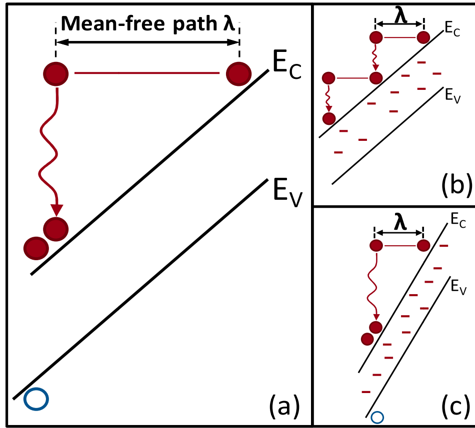

Fig. 16. Mechanism by which an impurity band can give rise to a breakdown walkout. (a) Impact ionization in the absence of unintentional impurities: electron gains enough energy to create an additional electron-hole pair. (b) Dopant impurities scatter with free carriers decreasing the mean-free path λ: the electron does not gain adequate energy to create an additional electron-hole pair. (c) To begin the avalanche process when there are impurities in the device, a higher band bending is required, i.e. a higher negative values of the voltage.

To trigger the avalanche process, an electron needs to gain enough energy from the field to create an additional electron-hole pair [Fig. 16(a)].

The density of electrons n^* having a sufficient energy to create electron-hole pairs is

$$n^* = n \cdot \exp\left(-\frac{d}{\lambda}\right)$$

where the total electron density n is multiplied by the probability that an electron has not collided in the distance d necessary to gain sufficient energy for the impact ionization [33]. As can be noticed, this probability depends on the mean-free path of an electron λ, given by

$$\lambda = \upsilon_{\text{th}} \tau_{\text{cn}}$$

where υ_{th} is the mean-square thermal velocity and τ_{cn} is the mean scattering time.

When a reverse bias is applied, the residual carbon acts as a deep acceptor, thus being negatively charged through the electron capture, as proven by C-DLTS and DLOS. C_N then increases the Coulomb scattering in the lattice, resulting in a decrease in the mean-free path of the free carriers [Fig. 16(b)] and a decrease in the density of excited electrons. Therefore, a higher (negative) BDV is required to trigger impact ionization once impurities are occupied by the electrons [Fig. 16(c)]. When a high negative bias is applied, C-impurities start gradually being negatively charged, with activation energy of the C_N defects. This leads to a decrease in the mean-free path, with a consequent increase in the avalanche voltage (breakdown walkout).

Hence, the increase in the scattering between free electrons and trapped electrons explains the breakdown walkout in the analyzed GaN-on-GaN vertical diodes.

IV. Conclusion

In summary, we demonstrated the avalanche capability, the breakdown walkout, and the role of the residual carbon in GaN-on-GaN vertical devices with polarization doping. The devices are avalanche capable and the BDV moves to higher negative when the devices are operated for a long time in reverse bias. The shift of the BDV is fully recoverable, demonstrating the presence of a not permanent breakdown walkout. The results of the temperature-dependent measurements suggest that the breakdown walkout originates from the reduction of mean-free path induced by the electron capture at C_N defects. The presence of carbon at the nitrogen sites was confirmed by C-DLTS and DLOS characterizations, and a model to explain the experimental data of the avalanche walkout process was proposed.

Recently, our preliminary investigations show no BDV walkout in the polarization-doped GaN p-n diodes with a carbon level below the detection limit, whose avalanche behavior was reported by Nomoto *et al.* [34]. These results will be described in detail in the near future. In short, we believe that the observed BDV walkout stems from the significant amount of carbon ($\sim N_d$), and it is not associated with polarization doping.

Acknowledgment

This research activity was partly funded by project "Novel vertical GaN-devices for next generation power conversion", NoveGaN (University of Padova), through the STARS CoG Grants call. The GaN p-n diodes were developed under the ARPAe SWITCHES Project at Cornell University, which made use of the Cornell Nanoscale Science and Technology Facilities (CNF) sponsored by the NSF NNCI Program (ECCS-1542081), and the Cornell Center for Materials Research Shared Facilities which are supported through the NSF MRSEC Program (DMR-1719875) and NSF MRI-1338010.

References

[1] K. Nomoto *et al.*, "GaN-on-GaN p-n power diodes with 3.48 kV and 0.95 mΩ-cm2: A record high figure-of-merit of 12.8 GW/cm2," in *IEDM Tech. Dig.*, Dec. 2016, pp. 9.7.1–9.7.4. doi: 10.1109/IEDM.2015.7409665.

[2] Z. Hu *et al.*, "1.1-kV vertical GaN p-n diodes with p-GaN regrown by molecular beam epitaxy," *IEEE Electron Device Lett.*, vol. 38, no. 8, pp. 1071–1074, Aug. 2017. doi: 10.1109/LED.2017.2720747.

[3] Z. Hu *et al.*, "Near unity ideality factor and Shockley-Read-Hall lifetime in GaN-on-GaN p-n diodes with avalanche breakdown," *Appl. Phys. Lett.*, vol. 107, no. 24, Dec. 2015, Art. no. 243501. doi: 10.1063/1.4937436.

[4] I. C. Kizilyalli, A. P. Edwards, O. Aktas, T. Prunty, and D. Bour, "Vertical power p-n diodes based on bulk GaN," *IEEE Trans. Electron Devices*, vol. 62, no. 2, pp. 414–422, Feb. 2015. doi: 10.1109/TED.2014.2360861.

[5] K. Nomoto *et al.*, "1.7-kV and 0.55-mΩÂ·cm^{2}GaN p-n diodes on bulk GaN substrates with avalanche capability," *IEEE Electron Device Lett.*, vol. 37, no. 2, pp. 161–164, Feb. 2016. doi: 10.1109/LED.2015.2506638.

[6] O. Aktas and I. C. Kizilyalli, "Avalanche capability of vertical GaN p-n junctions on bulk GaN substrates," *IEEE Electron Device Lett.*, vol. 36, no. 9, pp. 890–892, Sep. 2015. doi: 10.1109/LED.2015.2456914.

[7] H. G. Xing *et al.*, "Unique opportunity to harness polarization in GaN to override the conventional power electronics figure-of-merits," in *Proc. 73rd Annu. Device Res. Conf. (DRC)*, Jun. 2015, pp. 51–52. doi: 10.1109/DRC.2015.7175549.

[8] J. Simon, V. Protasenko, C. Lian, H. G. Xing, and D. Jena, "Polarization-induced hole doping in wide–band-gap uniaxial semiconductor heterostructures," *Science*, vol. 327, no. 5961, pp. 60–64, Jan. 2010. doi: 10.1126/science.1183226.

[9] M. Qi *et al.*, "High-voltage polarization-induced vertical heterostructure p-n junction diodes on bulk GaN substrates," in *Proc. 73rd Annu. Device Res. Conf. (DRC)*, Jun. 2015, pp. 31–32. doi: 10.1109/DRC.2015.7175537.

[10] W. Li *et al.*, "Enhancement of punch-through voltage in GaN with buried p-type layer utilizing polarization-induced doping," in *Proc. IEEE 30th Int. Symp. Power Semiconductor Devices ICs (ISPSD)*, May 2018, pp. 228–231. doi: 10.1109/ISPSD.2018.8393644.

[11] W. Li *et al.*, "Realization of GaN PolarMOS using selective-area regrowth by MBE and its breakdown mechanisms," *Jpn. J. Appl. Phys.*, vol. 58, May 2019, Art. no. SCCD15. doi: 10.7567/1347-4065/ab0f1b.

[12] C. De Santi *et al.*, "Demonstration of avalanche capability in polarization-doped vertical GaN pn diodes: Study of walkout due to residual carbon concentration," in *IEDM Tech. Dig.*, Dec. 2018, pp. 30.2.1–30.2.4. doi: 10.1109/IEDM.2018.8614568.

[13] J. L. Lyons, A. Janotti, and C. G. Van de Walle, "Effects of carbon on the electrical and optical properties of InN, GaN, and AlN," *Phys. Rev. B, Condens. Matter*, vol. 89, no. 3, Jan. 2014, Art. no. 035204. doi: 10.1103/PhysRevB.89.035204.

[14] D. Seghier and H. P. Gislason, "Electrical characterization of Mg-related energy levels and the compensation mechanism in GaN : Mg," *Phys. B, Condensed Matter*, vols. 273–274, pp. 46–49, Dec. 1999. doi: 10.1016/S0921-4526(99)00403-2.

[15] W. Götz, N. M. Johnson, J. Walker, D. P. Bour, and R. A. Street, "Activation of acceptors in Mg-doped GaN grown by metalorganic chemical vapor deposition," *Appl. Phys. Lett.*, vol. 667, pp. 667–669, Jan. 1996. doi: 10.1063/1.116503.

[16] P. Kozodoy, S. P. DenBaars, and U. K. Mishra, "Depletion region effects in Mg-doped GaN," *J. Appl. Phys.*, vol. 87, no. 2, pp. 770–775, Jan. 2000. doi: 10.1063/1.371939.

[17] I. C. Kizilyalli, A. P. Edwards, H. Nie, D. Disney, and D. Bour, "High voltage vertical GaN p-n diodes with avalanche capability," *IEEE Trans. Electron Devices*, vol. 60, no. 10, pp. 3067–3070, Oct. 2013. doi: 10.1109/TED.2013.2266664.

[18] K. G. McKay, "Avalanche breakdown in silicon," *Phys. Rev. J. Arch.*, vol. 94, no. 4, pp. 877–884, May 1954. doi: 10.1103/PhysRev.94.877.

[19] A. G. Chynoweth, "Ionization rates for electrons and holes in silicon," *Phys. Rev. J. Arch.*, vol. 109, pp. 1537–1540, Mar. 1958.

[20] G. Franssen, P. Perlin, and T. Suski, "Photocurrent spectroscopy as a tool for determining piezoelectric fields in $In_xGa_{1-x}N$/GaN multiple quantum well light emitting diodes," *Phys. Rev. B, Condens. Matter*, vol. 69, no. 4, Jan. 2004, Art. no. 045310. doi: 10.1103/PhysRevB.69.045310.

[21] T. Maeda *et al.*, "Franz-Keldysh effect in GaN p-n junction diode under high reverse bias voltage," *Appl. Phys. Lett.*, vol. 112, no. 25, Jun. 2018, Art. no. 252104. doi: 10.1063/1.5031215.

[22] W. L. Guo, R.-S. Huang, L. Z. Zheng, and Y. C. Song, "Walkout in p-n junctions including charge trapping saturation," *IEEE Trans. Electron Devices*, vol. 34, no. 8, pp. 1788–1794, Aug. 1987. doi: 10.1109/T-ED.1987.23152.

[23] P. C. Chao, M. Shur, M. Y. Kao, and B. R. Lee, "Breakdown walkout in AlAs/GaAs HEMTs," *IEEE Trans. Electron Devices*, vol. 39, no. 3, pp. 738–740, Mar. 1992. doi: 10.1109/16.123504.

[24] W.-B. Tang and Y.-M. Hsin, "Reversible off-state breakdown walkout in passivated AlGaAs/InGaAs PHEMTs," *IEEE Trans. Device Mater. Rel.*, vol. 6, no. 1, pp. 42–44, Mar. 2006. doi: 10.1109/TDMR.2006.870345.

[25] M. Caesar *et al.*, "Generation of traps in AlGaN/GaN HEMTs during RF-and DC-stress test," in *Proc. IEEE Int. Rel. Phys. Symp. (IRPS)*, Apr. 2012, pp. CD.6.1–CD.6.5. doi: 10.1109/IRPS.2012.6241883.

[26] M. Meneghini *et al.*, "Time- and field-dependent trapping in GaN-based enhancement-mode transistors with p-Gate," *IEEE Electron Device Lett.*, vol. 33, no. 3, pp. 375–377, Mar. 2012. doi: 10.1109/LED.2011.2181815.

[27] J. Osaka, Y. Ohno, S. Kishimoto, K. Maezawa, and T. Mizutani, "Deep levels in *n*-type AlGaN grown by hydride vapor-phase epitaxy on sapphire characterized by deep-level transient spectroscopy," *Appl. Phys. Lett.*, vol. 87, no. 22, Nov. 2005, Art. no. 222112. doi: 10.1063/1.2137901.

[28] K. Tanaka, M. Ishida, T. Ueda, and T. Tanaka, "Effects of deep trapping states at high temperatures on transient performance of AlGaN/GaN heterostructure field-effect transistors," *Jpn. J. Appl. Phys.*, vol. 52, Mar. 2013, Art. no. 04CF07.

[29] O. Mitrofanov and M. Manfra, "Poole-Frenkel electron emission from the traps in AlGaN/GaN transistors," *J. Appl. Phys.*, vol. 95, no. 11, pp. 6414–6419, May 2004. doi: 10.1063/1.1719264.

[30] D. V. Lang, "Deep-level transient spectroscopy: A new method to characterize traps in semiconductors," *J. Appl. Phys.*, vol. 45, no. 7, pp. 3023–3032, Jul. 1974.

[31] A. Chantre, G. Vincent, and D. Bois, "Deep-level optical spectroscopy in GaAs," *Phys. Rev. B, Condens. Matter*, vol. 23, no. 10, p. 5335, May 1981.

[32] A. Armstrong, T. A. Henry, D. D. Koleske, M. H. Crawford, and S. R. Lee, "Quantitative and depth-resolved deep level defect distributions in InGaN/GaN light emitting diodes," *Opt. Express*, vol. 20, pp. 812–821, Nov. 2012.

[33] R. S. Muller, T. I. Kamins, and M. Chan, *Device Electronics for Integrated Circuits*. Hoboken, NJ, USA: Wiley, 2003.

[34] K. Nomoto *et al.*, "Polarization-doped GaN p-n junction diodes with R_{on} of 0.1 mΩ cm^2 and V_{br} of > 1.2 kV," in *Proc. 42nd Int. Symp. Compound Semiconductors*, Santa Barbara, CA, USA, Jun./Jul. 2015.